Biochemistry and Biophysics Reports 21 (2020) 100717

Contents lists available at ScienceDirect

Biochemistry and Biophysics Reports

journal homepage: www.elsevier.com/locate/bbrep

Mitochondrial respiration of complex II is not lower than that of complex I in mouse skeletal muscle

Satoshi Maekawa[a], Shingo Takada[a,b,*], Takaaki Furihata[a], Arata Fukushima[a], Takashi Yokota[a], Shintaro Kinugawa[a]

[a] Department of Cardiovascular Medicine, Hokkaido University Graduate School of Medicine, Sapporo, Japan
[b] Faculty of Lifelong Sport, Department of Sports Education, Hokusho University, Ebetsu, Japan

ARTICLE INFO

Keywords:
Succinate dehydrogenase
Supercomplexes
Skeletal muscle
Oxidative phosphorylation

ABSTRACT

Skeletal muscle (SKM) requires a large amount of energy, which is produced mainly by mitochondria, for their daily functioning. Of the several mitochondrial complexes, it has been reported that the dysfunction of complex II is associated with several diseases, including myopathy. However, the degree to which complex II contributes to ATP production by mitochondria remains unknown. As complex II is not included in supercomplexes, which are formed to produce ATP efficiently, we hypothesized that complex II-linked respiration was lower than that of complex I. In addition, differences in the characteristics of complex I and II activity suggest that different factors might regulate their function. The isolated mitochondria from gastrocnemius muscle was used for mitochondrial respiration measurement and immunoblotting in male C57BL/6J mice. Student paired t-tests were performed to compare means between two groups. A univariate linear regression model was used to determine the correlation between mitochondrial respiration and proteins. Contrary to our hypothesis, complex II-linked respiration was not significantly less than complex I-linked respiration in SKM mitochondria (complex I vs complex II, 3402 vs 2840 pmol/[s × mg]). Complex I-linked respiration correlated with the amount of complex I incorporated in supercomplexes ($r = 0.727$, $p < 0.05$), but not with the total amount of complex I subunits. In contrast, complex II-linked respiration correlated with the total amount of complex II ($r = 0.883$, $p < 0.05$), but not with the amount of each complex II subunit. We conclude that both complex I and II play important roles in mitochondrial respiration and that the assembly of both supercomplexes and complex II is essential for the normal functioning of complex I and II in mouse SKM mitochondria.

1. Introduction

Skeletal muscle (SKM) requires a large amount of energy in the form of ATP to support daily activities, and the mitochondria within SKM play a key role in production of the necessary ATP. As tissues that require a large energy supply are vulnerable to mitochondrial dysfunction [1], perturbations in mitochondrial content or function might affect SKM function and consequently whole-body health [2]. It was reported that SKM mitochondrial function was impaired, not only in SKM diseases [3,4], but also in several diseases of other organs, e.g., type 2 diabetes, heart failure, and chronic obstructive pulmonary disease [5–9]. Moreover, reduced muscle mitochondrial function might contribute to age-associated muscle dysfunction [10].

Among the electron transport chain (ETC) complexes, complexes I, III, and IV form supermolecular structures called supercomplexes to enhance the efficiency of electron transfer, and this organization is strongly conserved across a wide range of species, i.e., fungi, plants, mice, and humans [11–13]. Unlike complexes I, III, and IV, complex II appears not to be a component of supercomplexes [14,15]. Complex II is a component of both the tricarboxylic acid (TCA) cycle and the ETC. In the context of the TCA cycle, complex II catalyzes the oxidation of succinate to fumarate in the mitochondrial matrix, with the reduction of ubiquinone to ubiquinol [16–18]. Thus, complex II is unique and important among eukaryotic ETC complexes.

Moreover, it was recently reported that complex II dysfunction may be associated with several diseases. For example, Birch-Machin et al. identified a family with complex II deficiency and late-onset neurodegenerative disease with progressive optic atrophy, ataxia, and myopathy [19]. They reported that their patients demonstrated a 50% decrease in complex II activity in SKM mitochondrial fractions, which

* Corresponding author. Department of Cardiovascular Medicine, Faculty of Medicine and Graduate School of Hokkaido University, Kita-15, Nishi-7, Kita-ku, Sapporo, 060-8638, Japan.
E-mail address: s-takada@hotmail.co.jp (S. Takada).

https://doi.org/10.1016/j.bbrep.2019.100717
Received 31 July 2019; Received in revised form 21 November 2019; Accepted 6 December 2019

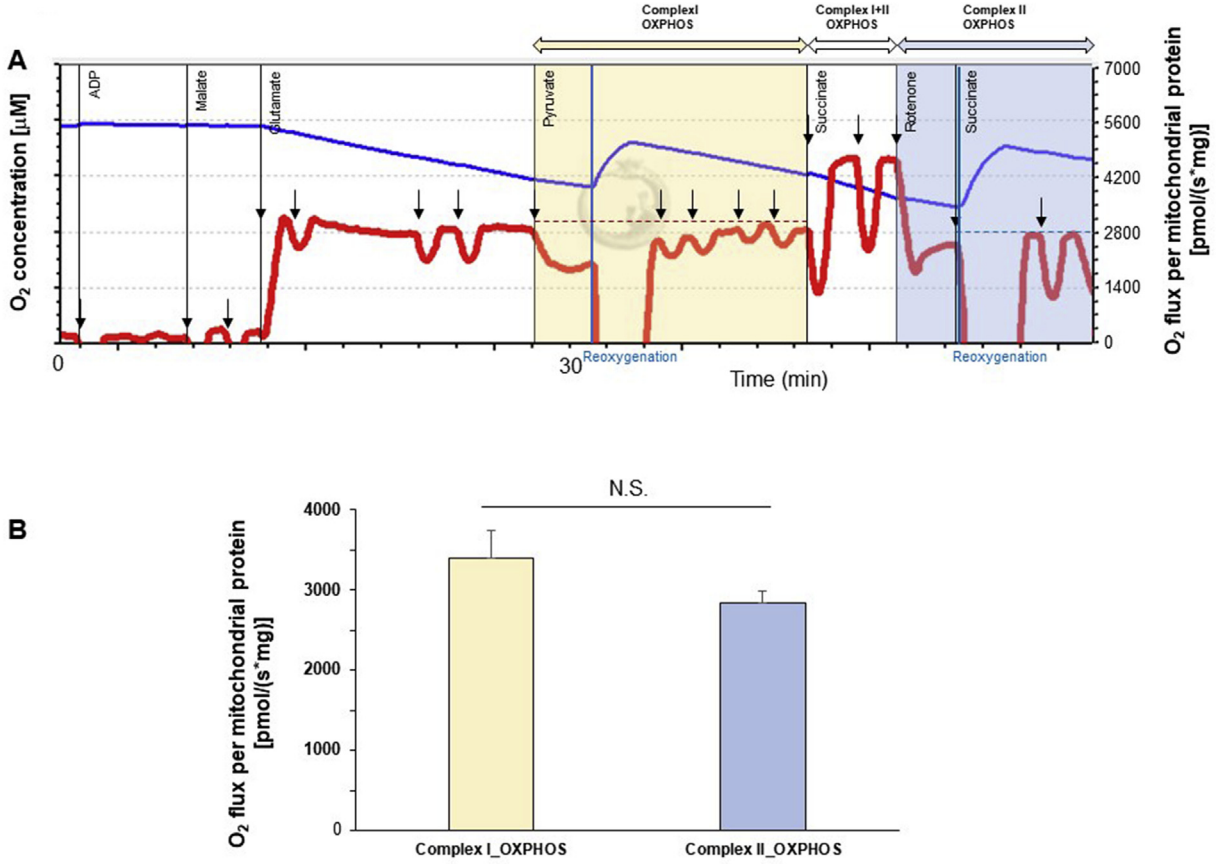

Fig. 1. Respiration of isolated skeletal muscle (SKM) mitochondria

A: Representative O_2 concentration (blue line) and O_2 flux (red line) measured in isolated SKM mitochondria by Oxygraph-2k high-resolution respirometry. After the addition of isolated mitochondria to the chamber of the respirometer, substrates, adenosine diphosphate (ADP), and inhibitors were added in the following order: (1) ADP (10 mmol/L), (2) malate (2 mmol/L/step), (3) glutamate (10 mmol/L/step), (4) pyruvate (5 mmol/L/step), (5) succinate (10 mmol/L/step), (6) rotenone (0.5 µmol/L), and (7) succinate (10 mmol/L/step). To measure maximum respiration without insufficiency of substrate, each substrate was added by stepwise titration until no further increase in O_2 flux was detected. In fact, it was necessary to add each substrate several times to achieve maximum respiration. The black arrows indicate the point at which each substrate was added. Yellow and blue horizontal dotted lines indicate the maximum respiration of complex I and complex II, respectively.

B: Comparison of maximum respiration measured in isolated SKM (gastrocnemius) mitochondria with substrates of complex I and II. Data are shown as means ± SE. N.S., not significant.

showed normal activity levels of complex I, complex III, and complex IV. In addition, Jackson et al. reported a patient with early progressive encephalomyopathy, in whom they found severe complex II deficiency owing to succinate dehydrogenase D (*Sdhd*) gene mutations [20]. The role of complex II has been reported in various diseases, ranging from cancer to neurodegenerative diseases. Indeed, complex II has been implicated in a diverse range of neurological dysfunction [21].

As described above, complex II has been widely studied [22]. However, the degree to which complex II contributes to ATP production by mitochondrial oxidative phosphorylation (OXPHOS) remains unclear. We hypothesize that complex II might not function to produce ATP to the same degree as complex I, as complex II is not a component of supercomplexes [23]. In this study, we therefore analyzed and compared the function of complex I and II in isolated SKM mitochondria and permeabilized SKM fibers.

In addition, it is reasonable to assume that the factors regulating the function of complexes I and II are different. That is, the function of complex II, which is not incorporated in supercomplexes, might be regulated by the expression level of complex II, whereas the function of complex I, which is a component of supercomplexes, might be affected by the assembly of supercomplexes. We tested this hypothesis by analyzing the expression levels of both complexes and their subunits.

2. Materials and methods

2.1. Experimental animals

Male C57BL/6J mice (9–12 weeks old; CLEA Japan, Tokyo) were bred in a pathogen-free environment and housed in an animal room maintained at 23–25 ˚C under controlled conditions on a 12-hr light/dark cycle. Diet (CE-2; CLEA Japan) and water were provided *ad libitum*. Heart samples were collected from the mice under deep anesthesia with Avertin (250 mg/kg body weight i.p.) before euthanasia.

2.2. Preparation of isolated mitochondria

Mitochondria were isolated from the SKM (gastrocnemius, soleus, and extensor digitorum longus [EDL]) of different mice (n = 8). The SKM was quickly harvested from the hind legs, and mitochondria were isolated as previously described [6,24,25]. Briefly, SKM tissues were minced on ice and then incubated for 2 min in mitochondrial isolation buffer (100 mmol/L sucrose, 100 mmol/L KCL, 1 mmol/L KH_2PO_4, 0.1 mmol/L EGTA, 0.2% bovine serum albumin (BSA), and 50 mmol/L Tris-HCl [pH 7.4]) containing 0.1 mg/mL proteinase (Sigma-Aldrich, St. Louis, MO). Tissues were gently homogenized with six strokes using a motor-driven Teflon pestle in a glass chamber. The homogenate was

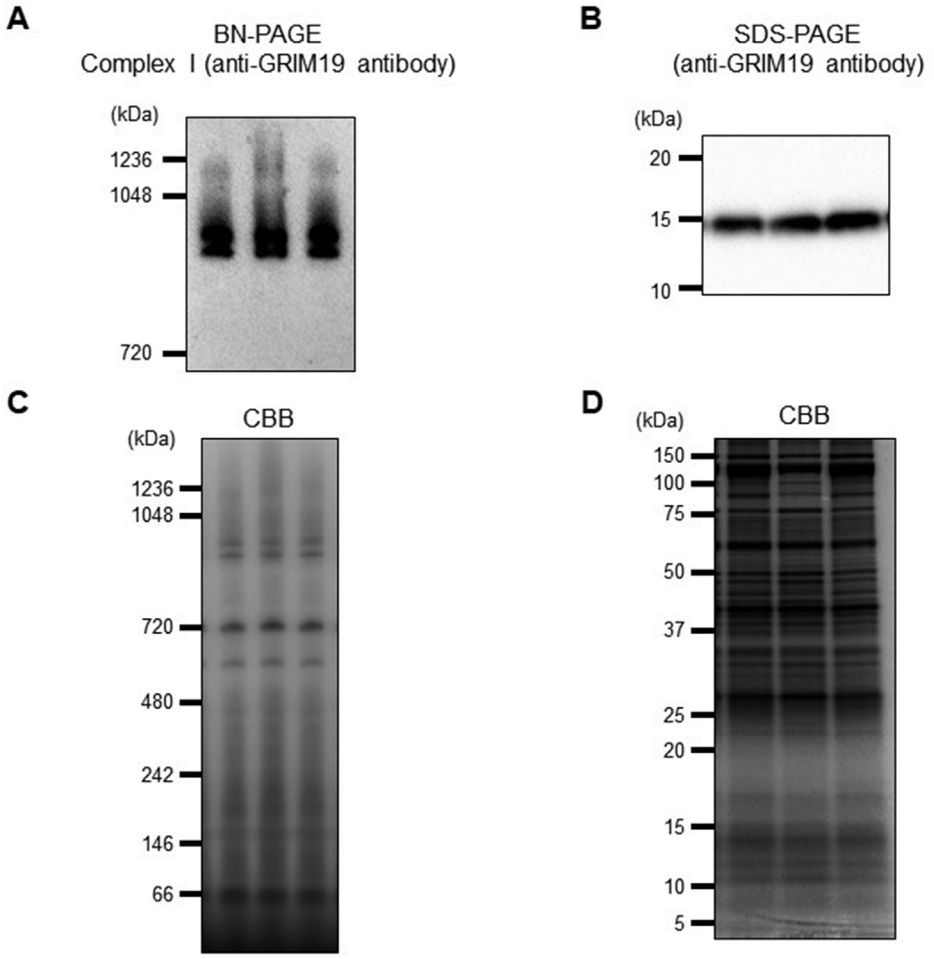

Fig. 2. Correlation between complex I-linked respiration and the amount of complex I incorporated into supercomplexes or the subunit of complex I
Mitochondria isolated from SKM (gastrocnemius) of different mice were used (n = 8).
A: BN-PAGE of isolated SKM mitochondria followed by immunoblotting with an antibody against GRIM19.
B: SDS-PAGE of isolated SKM mitochondria followed by immunoblotting with an antibody against GRIM19 (17 kDa).
C: BN-PAGE followed by CBB staining showing the amount of proteins loaded onto each lane.
D: SDS-PAGE followed by CBB staining showing the proteins loaded in each lane.
E: Correlation between the content of complex I involved in supercomplexes analyzed by immunoblotting using an antibody against GRIM19 and complex I-linked respiration.
F: Correlation between the content of the GRIM19 subunit and complex I-linked respiration.
G: Correlation between the content of complex I analyzed by immunoblotting with an antibody against GRIM19 and the content of the GRIM19 subunit.
Sizes of the molecular mass markers are indicated on the left in kDa. The Pearson correlation coefficient and *P*-value are shown. BN-PAGE, blue native-polyacrylamide gel electrophoresis; SDS-PAGE, sodium dodecyl sulfate-polyacrylamide gel electrophoresis; CBB, Coomassie Brilliant Blue; N.S., not significant.

centrifuged at 700 *g* for 10 min. The supernatant was then centrifuged at 10,000 *g* for 10 min, and the pellet was washed and centrifuged at 7000 *g* for 3 min. The final pellet was suspended in suspension buffer (containing 225 mmol/L mannitol, 75 mmol/L sucrose, 10 mmol/L Tris, and 0.1 mmol/L EDTA [pH 7.4]). Finally, the mitochondrial protein concentration was measured using the bicinchoninic acid assay.

2.3. Immunoblotting

Immunoblotting was performed as described previously [26]. Samples of mitochondrial protein from SKM tissues were separated by sodium dodecyl sulfate-polyacrylamide gel electrophoresis (SDS-PAGE) and transferred to a polyvinylidene fluoride (PVDF) membrane (Bio-Rad, Hercules, CA). The membrane was blocked for 1 h at room temperature in Tris-buffered saline containing 0.1% Tween 20 (TBS-T) buffer containing 3% milk, and then incubated with the primary antibodies (SDHA, SDHB, SDHC, SDHD, and GRIM19; Abcam, Cambridge, MA) at a dilution of 1:1000 overnight at 4 °C. After three washings with TBS-T, the membrane was incubated with a horseradish peroxide-conjugated secondary antibody at a dilution of 1:5000 for 1 h at room temperature. After washing, the membrane was developed with ECL, ECL Prime, or SuperSignal West Dura Reagent (GE Healthcare Life Sciences, Piscataway, NJ) and then processed for detection with ChemiDoc XRS+ (Bio-Rad). The density of the band signals was quantified using Image J software (U.S. National Institutes of Health, Bethesda, MD). The expression levels of proteins are shown as values normalized to total mitochondrial protein levels (Coomassie Brilliant Blue, CBB staining).

2.4. Blue native polyacrylamide gel electrophoresis (BN-PAGE)

BN-PAGE was performed as described previously [13]. The proteins from SKM mitochondria were extracted with 5% digitonin (Invitrogen, Carlsbad, CA; protein:detergent ratio of 1:10) and 4 × buffer on ice for 30 min. After centrifugation at 10,000 *g* for 10 min at 4 °C, the supernatants were collected. The remaining lysate was combined with

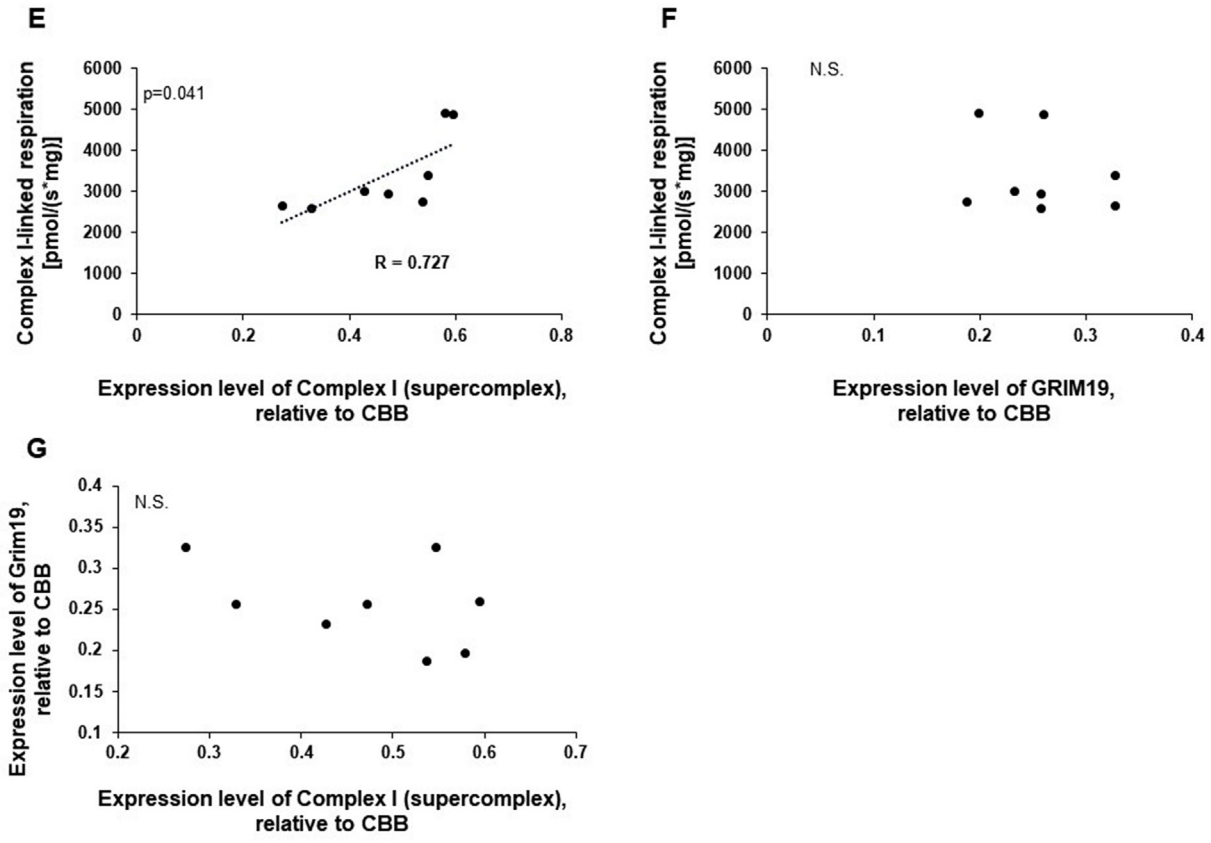

Fig. 2. (*continued*)

Coomassie blue G-250 dye (Invitrogen; protein:detergent ratio of 1:10) and added to 3%–12% NativePAGE Novex Bis-Tris Gel (Invitrogen), then separated by electrophoresis using Anode and Cathode buffer (Invitrogen) at 10 mA for 1 h and at 150 V for 2 h on ice. The protein complex in the samples after the electrophoresis was denatured by denaturing buffer (Tris [20 mmol], glycine [200 mmol], 1% SDS). The gels were then transferred by electroblotting to PVDF membranes (Bio-Rad) using transfer buffer at 25 V for 2 h.

2.5. Measurement of mitochondrial OXPHOS capacity

The mitochondrial respiratory capacity was measured in isolated mitochondria at 37 °C with a high-resolution respirometer (Oxygraph-2k; Oroboros Instruments, Innsbruck, Austria) [13,27–29]. The respirometer chamber was filled with 2 mL of MiR05 medium, and then the isolated mitochondria (approx. 30–100 μg) were added, followed by the substrates, ADP, and inhibitors in the following order: (1) ADP (10 mmol/L), (2) malate (2 mmol/L/step), (3) glutamate (10 mmol/L/step), (4) pyruvate (5 mmol/L/step), (5) succinate (10 mmol/L/step), (6) rotenone (0.5 μmol/L), and (7) succinate 10 (mmol/L/step). The O_2 consumption rates (i.e., respiratory rates) were expressed as O_2 flux normalized to the mitochondrial protein concentration (μg/μL). DatLab software (Oroboros Instruments) was used for data acquisition and data analysis. O_2 flux per mitochondrial protein was measured after the addition of ADP, malate, glutamate, and pyruvate, and after the addition of succinate and rotenone, as complex I-linked and complex II-linked respiration, respectively. To measure maximum respiration under conditions of sufficient substrate, each substrate was added by stepwise titration until no further increase in O_2 flux was observed.

2.6. Measurement of O_2 consumption in isolated mitochondria with inhibitors of complex I and II

The mitochondrial O_2 consumption in states 3 and 4 was measured in isolated mitochondria at 37 °C with a high-resolution respirometer (Oxygraph-2k; Oroboros Instruments, Innsbruck, Austria). To measure complex I-linked and II-linked respiration more accurately, we added rotenone and malonate as inhibitors of complex I and II, respectively. The respirometer chamber was filled with 2 mL of MiR05 medium, and then the isolated mitochondria (approximately 30–100 μg) were added, followed by the substrates, ADP, and inhibitors in the following protocol. O_2 consumption rates (i.e., respiratory rates) were expressed as O_2 flux normalized to the mitochondrial protein concentration (μg/μL).

Protocol for complex I: (1) ADP (10 mmol/L), (2) malonate (5 mmol/L), (3) malate (2 mmol/L/step), (4) glutamate (10 mmol/L/step), (5) pyruvate (5 mmol/L/step), and (6) oligomycin (10 mmol/L).

Protocol for complex II: (1) ADP (10 mmol/L), (2) rotenone (0.5 μmol/L), (3) succinate (10 mmol/L/step), and (4) oligomycin (10 mmol/L).

2.7. Preparation of permeabilized fibers

After the careful dissection of muscle tissue, fiber bundles were permeabilized by gentle agitation for 30 min in an ice-cold relaxing BIOPS solution (in mmol/L: CaK_2EGTA [2.77], K_2EGTA [7.23], Na_2ATP [5.77], $MgCl_2 \cdot 6H_2O$ [6.56], taurine [20], Na_2phosphocreatine [15], imidazole [20], dithiothreitol [0.5], MES hydrate [50], pH 7.1) with saponin (50 μg/mL), as previously described [27,30]. After permeabilization, the fibers were rinsed twice by agitation for 10 min in an ice-cold respiration medium, MiR05 (in mmol/L: sucrose [110], K-lactobionate [60], EGTA [0.5], $MgCl_2$ [3], taurine [20], KH_2PO_4 [10], 4-(2-hydroxyethyl)-piperazineethanesulfonic acid [20]), 1% BSA [pH 7.1]).

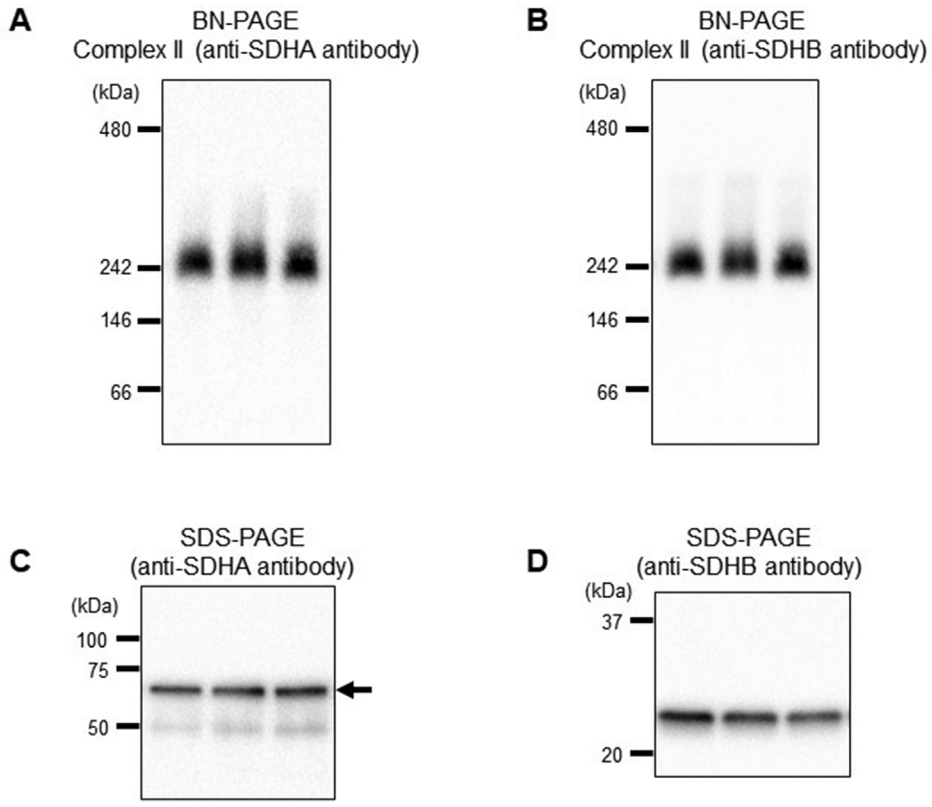

Fig. 3. Correlation between complex II-linked respiration and the content of complex II or the subunit of complex II
Mitochondria isolated from SKM (gastrocnemius) of different mice were used (n = 8).
A: BN-PAGE of isolated SKM mitochondria followed by immunoblotting with an antibody against SDHA.
B: BN-PAGE of isolated SKM mitochondria followed by immunoblotting with an antibody against SDHB.
C: SDS-PAGE of isolated SKM mitochondria followed by immunoblotting with an antibody against SDHA (black arrow, 70 kDa).
D: SDS-PAGE of isolated SKM mitochondria followed by immunoblotting with an antibody against SDHB (28 kDa).
E: Correlation between the content of complex II analyzed by immunoblotting using an antibody against SDHA and complex II-linked respiration.
F: Correlation between the content of complex II analyzed by immunoblotting using an antibody against SDHB and complex II-linked respiration.
G: Correlation between the content of the SDHA subunit and complex II-linked respiration.
H: Correlation between the content of the SDHB subunit and complex II-linked respiration.
I: Correlation between the content of complex II and that of the SDHA subunit.
J: Correlation between the content of complex II and that of the SDHB subunit.
Sizes of molecular mass markers are indicated on the left in kDa. The Pearson correlation coefficient (R) and *P*-values are shown. BN-PAGE, blue native-polyacrylamide gel electrophoresis; SDS-PAGE, sodium dodecyl sulfate-polyacrylamide gel electrophoresis; N.S., not significant.

2.8. Measurement of mitochondrial OXPHOS capacity in permeabilized fibers

Mitochondrial respiratory capacity was measured in permeabilized fibers at 37 °C with a high-resolution respirometer (Oxygraph-2k) [27,30]. The respirometer chamber was filled with 2 mL of MiR05 medium and permeabilized fibers (approximately 1.5–3.0 mg of gastrocnemius muscle) were added, followed by the substrates, ADP, and inhibitors in the following order: (1) ADP (10 mmol/L), (2) malate (2 mmol/L/step), (3) glutamate (10 mmol/L/step), (4) pyruvate (5 mmol/L/step), (5) succinate (10 mmol/L/step), (6) rotenone (0.5 μmol/L), and (7) succinate (10 mmol/L/step). We tested the integrity of the outer mitochondrial membrane by adding cytochrome *c*, and the data was disregarded when the increase in the oxygen consumption rate was > 10% as a sign of damaged outer mitochondrial membranes. The O_2 consumption rates (i.e., respiratory rates) were expressed as O_2 flux normalized to the muscle weight (pmol/sec/mg wet weight of muscle tissue). DatLab software (Oroboros Instruments) was used for data acquisition and data analysis. We measured O_2 flux per muscle weight after the addition of ADP, malate, glutamate, and pyruvate and after the addition of succinate and rotenone as complex I-linked and II-linked respiration, respectively.

2.9. Statistical analysis

Data are expressed as the mean ± standard error of the mean (SE). Student paired *t*-tests were performed to compare means between two groups. A univariate linear regression model was used to determine the correlation between mitochondrial respiration and proteins. *P*-values less than 0.05 were considered to indicate a statistically significant difference between groups.

3. Results

3.1. Comparable levels of mitochondrial complex I-linked and complex II-linked respiration in state 3

We first measured mitochondrial respiration in isolated mouse SKM (gastrocnemius) mitochondria using an Oxygraph-2k high-resolution respirometer. Fig. 1A shows the O_2 flux and O_2 concentration of representative raw data. We used malate, glutamate, and pyruvate as substrates for complex I, succinate as the substrate for complex II, and rotenone as the inhibitor for complex I. If necessary, substrates were added by stepwise titration until the maximum respiration was achieved. In fact, we needed to add each substrate several times to

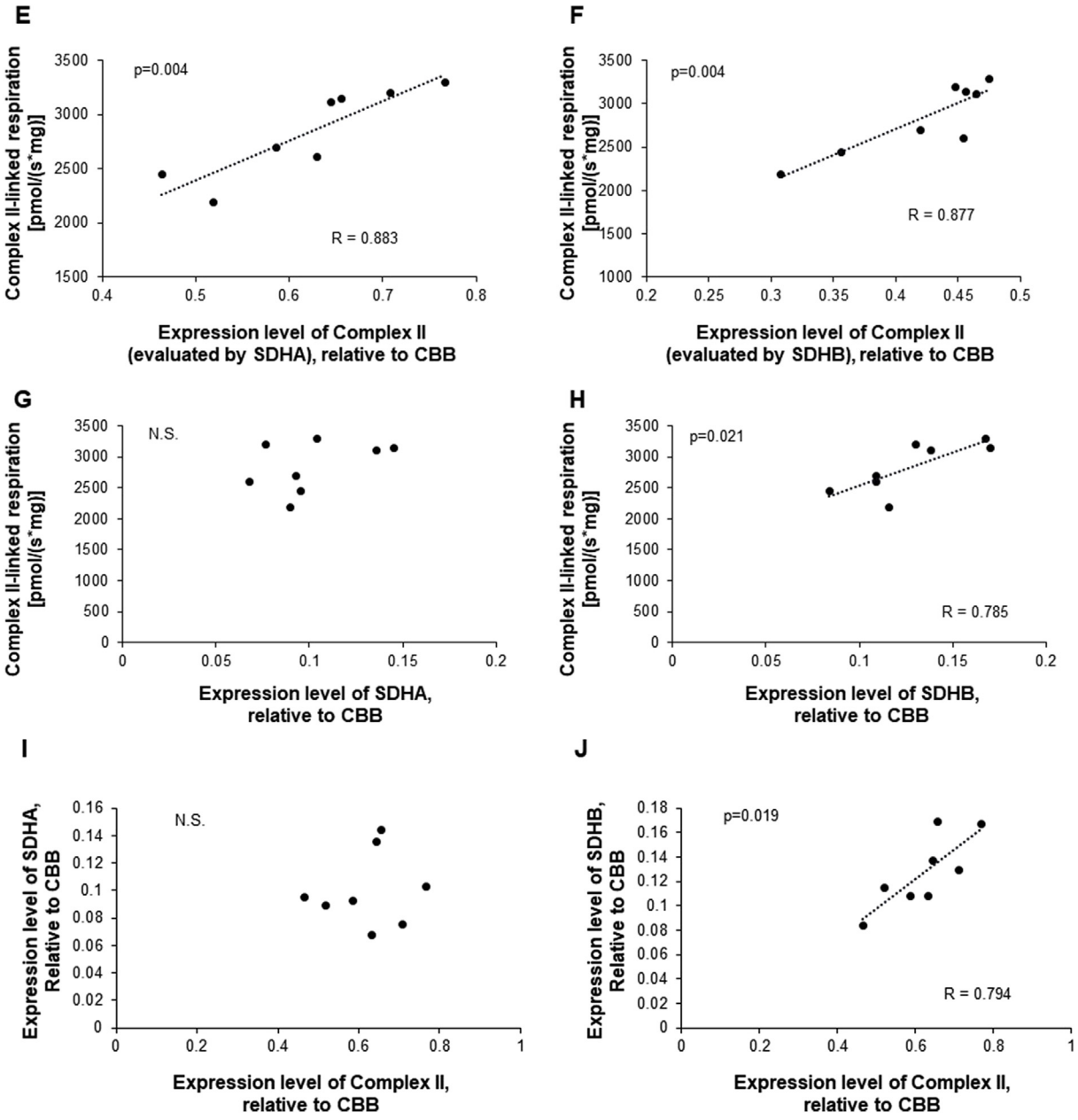

Fig. 3. (*continued*)

achieve maximum respiration (Fig. 1A). Contrary to our expectations, the level of complex II-linked respiration in state 3 was not lower than that of complex I-linked respiration ($P = 0.06$) (Fig. 1B). We measured respiration of mitochondrial complex I after addition of malonate (an inhibitor of complex II) or complex II after addition of rotenone (an inhibitor of complex I). Similar to our data in Fig. 1, complex II-linked respiration was equivalent to that of complex I ($P = 0.26$) (suppl. Fig.1). Moreover, we added malonate to quantify complex I-linked respiration more accurately. Correspondingly, complex II-linked respiration was equivalent to that of complex I ($P = 0.09$) (suppl. Fig. 2). Similar results were obtained when we measured mitochondrial respiration using permeabilized fibers instead of isolated mitochondria. The level of complex II-linked respiration in state 3 in permeabilized fibers was also comparable to that of complex I-linked respiration ($P = 0.12$) (suppl. Fig. 3B). On the other hand, with respect to the respiratory control ratio (RCR), complex I was significantly superior to complex II (suppl. Fig. 3C). This reflected the result that the level of complex II-linked respiration in state 4 was significantly higher than that of complex I (suppl. Fig. 3A). Similar results were observed when we investigated mitochondrial respiration of other muscles (soleus and extensor digitorum longus [EDL]) (suppl. Fig. 4 and 5).

3.2. Amount of complex I incorporated into supercomplexes significantly correlated with complex I-linked respiration

Next, we investigated our hypothesis that the content of complex I correlates with the level of complex I-linked respiration in state 3. For this purpose, we analyzed the expression level of complex I by BN-PAGE analysis followed by immunoblotting using antibodies against a complex I subunit (GRIM19). The bands detected with an antibody against GRIM19 were ladder-like bands (Fig. 2A). These bands might indicate complex I involved in supercomplexes, as the same bands were found when we used an antibody against a complex III subunit (UQCRC2) (data not shown). In addition, whereas the amount of complex I that was a constituent of supercomplexes significantly correlated with complex I-linked respiration (Fig. 2E), the amount of the

complex I subunit (GRIM19) was not correlated with respiration (Fig. 2B and F).

Amount of complex I incorporated into supercomplexes did not significantly correlate with the total amount of the complex I subunit.

From our results described above, we assumed that the amount of supercomplexes was not correlated with the total amount of the complex I subunit (GRIM19). As expected, a significant correlation was not found between the amount of complex I that was included in supercomplexes and the total amount of the complex I subunit (GRIM19) (Fig. 2G).

3.3. Complex II content significantly correlated with complex II-linked respiration

We next investigated whether the content of complex II correlated with complex II-linked respiration in state 3. The expression level of complex II was analyzed by BN-PAGE followed by immunoblotting using antibodies against SDHA (Fig. 3A) or SDHB (Fig. 3B). As the bands observed with antibodies against SDHC or SDHD were not as clear as the bands detected with antibodies against SDHA or SDHB (data not shown), we chose to use antibodies against SDHA and SDHB to analyze the expression levels of complex II. Regardless of which antibody was used, the content of complex II significantly correlated with complex II-linked respiration (Fig. 3E and F).

Amount of the complex II subunit (SDHB) in supercomplexes correlated with complex II-linked respiration.

Following our above-described finding that the total amount of complex II significantly correlated with complex II-linked respiration, we investigated whether the amounts of complex II subunits (SDHA and SDHB) correlated with complex II-linked respiration in state 3. The expression levels of the SDHA subunit and SDHB subunit were analyzed by SDS-PAGE followed by immunoblotting using antibodies against SDHA (Fig. 3C) and SDHB (Fig. 3D), respectively. The results showed that the amount of the SDHB subunit significantly correlated with complex II-linked respiration (Fig. 3H), but no correlation was observed between the amount of the SDHA subunit and complex II-linked respiration (Fig. 3G).

3.4. Amount of the SDHB subunit correlated with the amount of complex II

As the content of the SDHB subunit significantly correlated with complex II-linked respiration, we were interested in whether the amount of complex II subunits and SDHA and SDHB within complex II subunits correlated with total amounts of complex II. As illustrated in Fig. 3I and J, the amount of the SDHB subunit within complex II significantly correlated with total amounts of complex II, whereas the amount of the SDHA subunit did not.

4. Discussions

The contraction of muscle fibers requires a large amount of energy in the form of ATP produced mainly by mitochondria. Tissues with a high energy demand, such as SKM, heart, and the nervous system, are most vulnerable to mitochondrial dysfunction [1]. We therefore considered that it would be meaningful to analyze the ability of mitochondria to produce ATP in SKM. As it was previously reported that the rate of ATP production significantly correlated with the amount of mitochondrial respiration in state 3 [31,32], in this study we analyzed complex I-linked and II-linked respiration in state 3.

We measured complex I-linked and II-linked respiration in state 3 and compared them in isolated mouse SKM mitochondria. Contrary to our expectations, our results demonstrated that the level of complex II-linked respiration in state 3 was comparable to that of complex I-linked respiration (Fig. 1). A similar result was obtained when we measured respiration in state 3 using permeabilized fibers instead of isolated mitochondria (suppl. Fig. 2). On the other hand, the RCR of complex I was significantly higher than that of complex II (suppl. Fig. 3, 4, and 5). We considered the meaning of this dissociation between respiration in state 3 and RCR. Based on reports demonstrating that the rate of ATP production was significantly correlated with mitochondrial respiration in state 3 in isolated mitochondria [31,32], our results showing that the level of complex II-linked respiration in state 3 was comparable to that of complex I suggested that complex II might produce ATP at a level comparable to complex I per mitochondria. The higher RCR of complex I might reflect the ability of individual complex Is to produce ATP more efficiently in comparison to individual complex IIs by forming supercomplexes; e.g., Quarato et al. reported different activities of complex IV depending on whether complex I was linked or not [33]. Although we did not investigate protein amounts in this study, it has been reported that the complex I:II protein ratio is 1:1.5–3 [34–37]; that is, that the amount of complex II is higher than that of complex I. From these findings, we speculate that the inefficiency of individual complex IIs to produce ATP compared with supercomplexes might be compensated for by the amount of complex II, and consequently, the complex II-linked respiration in state 3 per mitochondria is equivalent to that of complex I, that is, ATP production by complex II might be comparable to that of complex I per mitochondria. Therefore, we believe it is worth evaluating the function of complex II as well as that of complex I when estimating the mitochondrial ability to produce ATP.

We observed that complex I-linked respiration in state 3 significantly correlated with the expression level of complex I incorporated into supercomplexes, but not with that of a complex I subunit (GRIM19) (Fig. 2E and F). These results suggested that complex I-linked respiration might be affected by the amount of supercomplexes rather than the amount of the complex I subunit. In addition, no correlation was observed between the amount of supercomplexes and the content of complex I subunits (Fig. 2G). These results indicate that the amount of supercomplexes might not be regulated by the content of complex I subunits and there might be some other factors regulating the assembly of supercomplexes.

The level of complex–II–linked respiration in state 3 was significantly correlated with the expression of complex II (Fig. 3E and F). This result indicates that supercomplex assembly is essential for complex II to function properly. Although complex II-linked respiration in state 3 was correlated with the content of the SDHB subunit, no correlation was found between respiration and the content of the SDHA subunit (Fig. 3G and H). Moreover, the content of SDHB subunits correlated with the content of complex II, but the content of SDHA subunits did not correlate with complex II content (Fig. 3I and J). From these results, we speculate that the SDHA and SDHB subunits may not be entirely equivalent in terms of their behavior or roles in mitochondria. That is, the ratio of the SDHA subunit included in complex II to the total amount of the SDHA subunit may be lower than the corresponding ratio for the SDHB subunit. In fact, it has been reported that the SDHA subunit might not only be a component of complex II but might be a component of mitochondrial ATP-sensitive potassium channels [38].

From these results, not only complex I-derived but also complex II-derived respiration should be analyzed when measuring mitochondrial function. Moreover, the question of whether disassembly of supercomplexes or complex II is associated with diseases induced by mitochondrial dysfunction should be investigated.

5. Conclusions

We conclude that both complex I and II play important roles in mitochondrial respiration and that the assembly of both supercomplexes and complex II is essential for the normal functioning of complex I and II in mouse SKM mitochondria.

CRediT authorship contribution statement

Satoshi Maekawa: Formal analysis, Writing - original draft. **Shingo**

Takada: Conceptualization, Data curation, Formal analysis, Funding acquisition, Investigation, Methodology, Project administration, Resources, Supervision, Validation, Visualization, Writing - original draft, Writing - review & editing. **Takaaki Furihata:** Formal analysis. **Shintaro Kinugawa:** Conceptualization, Funding acquisition, Resources, Supervision, Writing - review & editing.

Declaration of competing interest

None.

Acknowledgments

The authors thank Yuki Kimura, Noriko Ikeda and Miwako Yamane for their technical assistance, and Misaki Kihara, Naoko Toshiro, Tsukusu Yamanaka, and Misato Kobayashi for secretarial support, and H.A. Popiel for her critical reading of the manuscript.

Abbreviations

SKM	skeletal muscle
SDH	succinate dehydrogenase
ETC	electron transport chain
BN-PAGE	Blue Native-Polyacrylamide Gel Electrophoresis
CBB	Coomassie Brilliant Blue
OXPHOS	oxidative phosphorylation

Appendix A. Supplementary data

Supplementary data to this article can be found online at https://doi.org/10.1016/j.bbrep.2019.100717.

Funding

This work was supported in part by grants from Japanese Grant-In-Aid for Scientific Research (JP17H04758 [to S.T.], and 18H03187 [to S.K.]), Grant-in-Aid for Challenging Exploratory Research (19K22791 [to S.T.], the Japan Foundation for Applied Enzymology (to S.T.), a Hokkaido Heart Association Grant for Research (to S.T.), the MSD Life Science Foundation (to S.T.), the Uehara Memorial Foundation (to S.T.), the Cardiovascular Research Fund, Tokyo, Japan (to S.T.), the Fukuda Memorial Foundation for Medical Research (to S.T.), a Kimura Memorial Heart Foundation Research Grant for 2017 (to S.T.), the SENSHIN Medical Research Foundation (to S.T.), the Nakatomi Foundation (to S.T.), the Japan Heart Foundation (to S.T.), a Sasakawa Scientific Research Grant from The Japan Science Society (to S.T.), and the Center of Innovation Program from the Japan Science and Technology Agency.

Availability of data and materials

The datasets generated during and/or analyzed during the current study are available from the corresponding author upon reasonable request.

Consent for publication

Not applicable.

Disclosures

The authors state that there are no disclosures to provide.

Ethics approval and consent to participate

All procedures and animal care were approved by our institutional animal research committee and conformed to the Animal Care Guidelines for the Care and Use of Laboratory Animals at Hokkaido University Graduate School of Medicine. The procedures and animal care were also in accordance with the relevant national and international guidelines and the Guide for the Care and Use of Laboratory Animals published by the U.S. National Institutes of Health.

References

[1] G.H. Renkema, S.B. Wortmann, R.J. Smeets, H. Venselaar, M. Antoine, G. Visser, T. Ben-Omran, L.P. van den Heuvel, H.J. Timmers, J.A. Smeitink, R.J. Rodenburg, SDHA mutations causing a multisystem mitochondrial disease: novel mutations and genetic overlap with hereditary tumors, Eur. J. Hum. Genet. 23 (2015) 202–209.
[2] A.P. Russell, V.C. Foletta, R.J. Snow, G.D. Wadley, Skeletal muscle mitochondria: a major player in exercise, health and disease, Biochim. Biophys. Acta 1840 (2014) 1276–1284.
[3] S.M. Gehrig, V. Mihaylova, S. Frese, S.M. Mueller, M. Ligon-Auer, C.M. Spengler, J.A. Petersen, C. Lundby, H.H. Jung, Altered skeletal muscle (mitochondrial) properties in patients with mitochondrial DNA single deletion myopathy, Orphanet J. Rare Dis. 11 (2016) 105.
[4] H. Lemieux, F. Boemer, G. van Galen, D. Serteyn, H. Amory, E. Baise, D. Cassart, G. van Loon, C. Marcillaud-Pitel, D.M. Votion, Mitochondrial function is altered in horse atypical myopathy, Mitochondrion 30 (2016) 35–41.
[5] R.A. Rabinovich, R. Bastos, E. Ardite, L. Llinas, M. Orozco-Levi, J. Gea, J. Vilaro, J.A. Barbera, R. Rodriguez-Roisin, J.C. Fernandez-Checa, J. Roca, Mitochondrial dysfunction in COPD patients with low body mass index, Eur. Respir. J. 29 (2007) 643–650.
[6] T. Yokota, S. Kinugawa, K. Hirabayashi, S. Matsushima, N. Inoue, Y. Ohta, S. Hamaguchi, M.A. Sobirin, T. Ono, T. Suga, S. Kuroda, S. Tanaka, F. Terasaki, K. Okita, H. Tsutsui, Oxidative stress in skeletal muscle impairs mitochondrial respiration and limits exercise capacity in type 2 diabetic mice, Am. J. Physiol. Heart Circ. Physiol. 297 (2009) H1069–H1077.
[7] S. Takada, S. Kinugawa, K. Hirabayashi, T. Suga, T. Yokota, M. Takahashi, A. Fukushima, T. Homma, T. Ono, M.A. Sobirin, Y. Masaki, W. Mizushima, T. Kadoguchi, K. Okita, H. Tsutsui, Angiotensin II receptor blocker improves the lowered exercise capacity and impaired mitochondrial function of the skeletal muscle in type 2 diabetic mice, J. Appl. Physiol. 114 (1985) 844–857 2013.
[8] S. Takada, K. Hirabayashi, S. Kinugawa, T. Yokota, S. Matsushima, T. Suga, T. Kadoguchi, A. Fukushima, T. Homma, W. Mizushima, Y. Masaki, T. Furihata, R. Katsuyama, K. Okita, H. Tsutsui, Pioglitazone ameliorates the lowered exercise capacity and impaired mitochondrial function of the skeletal muscle in type 2 diabetic mice, Eur. J. Pharmacol. 740 (2014) 690–696.
[9] S. Kinugawa, S. Takada, S. Matsushima, K. Okita, H. Tsutsui, Skeletal muscle abnormalities in heart failure, Int. Heart J. 56 (2015) 475–484.
[10] K.R. Short, M.L. Bigelow, J. Kahl, R. Singh, J. Coenen-Schimke, S. Raghavakaimal, K.S. Nair, Decline in skeletal muscle mitochondrial function with aging in humans, Proc. Natl. Acad. Sci. U. S. A. 102 (2005) 5618–5623.
[11] N.V. Dudkina, H. Eubel, W. Keegstra, E.J. Boekema, H.P. Braun, Structure of a mitochondrial supercomplex formed by respiratory-chain complexes I and III, Proc. Natl. Acad. Sci. U. S. A. 102 (2005) 3225–3229.
[12] M.G. Rosca, E.J. Vazquez, J. Kerner, W. Parland, M.P. Chandler, W. Stanley, H.N. Sabbah, C.L. Hoppel, Cardiac mitochondria in heart failure: decrease in respirasomes and oxidative phosphorylation, Cardiovasc. Res. 80 (2008) 30–39.
[13] S. Takada, Y. Masaki, S. Kinugawa, J. Matsumoto, T. Furihata, W. Mizushima, T. Kadoguchi, A. Fukushima, T. Homma, M. Takahashi, S. Harashima, S. Matsushima, T. Yokota, S. Tanaka, K. Okita, H. Tsutsui, Dipeptidyl peptidase-4 inhibitor improved exercise capacity and mitochondrial biogenesis in mice with heart failure via activation of glucagon-like peptide-1 receptor signalling, Cardiovasc. Res. 111 (2016) 338–347.
[14] N.V. Dudkina, S. Sunderhaus, E.J. Boekema, H.P. Braun, The higher level of organization of the oxidative phosphorylation system: mitochondrial supercomplexes, J. Bioenerg. Biomembr. 40 (2008) 419–424.
[15] L.A. Gomez, J.S. Monette, J.D. Chavez, C.S. Maier, T.M. Hagen, Supercomplexes of the mitochondrial electron transport chain decline in the aging rat heart, Arch. Biochem. Biophys. 490 (2009) 30–35.
[16] J. Rutter, D.R. Winge, J.D. Schiffman, Succinate dehydrogenase - assembly, regulation and role in human disease, Mitochondrion 10 (2010) 393–401.
[17] A.P. Wojtovich, C.O. Smith, C.M. Haynes, K.W. Nehrke, P.S. Brookes, Physiological consequences of complex II inhibition for aging, disease, and the mKATP channel, Biochim. Biophys. Acta 1827 (2013) 598–611.
[18] A. Stepanova, Y. Shurubor, F. Valsecchi, G. Manfredi, A. Galkin, Differential susceptibility of mitochondrial complex II to inhibition by oxaloacetate in brain and heart, Biochim. Biophys. Acta 1857 (2016) 1561–1568.
[19] M.A. Birch-Machin, R.W. Taylor, B. Cochran, B.A. Ackrell, D.M. Turnbull, Late-onset optic atrophy, ataxia, and myopathy associated with a mutation of a complex II gene, Ann. Neurol. 48 (2000) 330–335.
[20] C.B. Jackson, J.M. Nuoffer, D. Hahn, H. Prokisch, B. Haberberger, M. Gautschi, A. Haberli, S. Gallati, A. Schaller, Mutations in SDHD lead to autosomal recessive encephalomyopathy and isolated mitochondrial complex II deficiency, J. Med. Genet. 51 (2014) 170–175.
[21] C. Eng, M. Kiuru, M.J. Fernandez, L.A. Aaltonen, A role for mitochondrial enzymes in inherited neoplasia and beyond, Nat. Rev. Cancer 3 (2003) 193–202.
[22] A. Bezawork-Geleta, J. Rohlena, L. Dong, K. Pacak, J. Neuzil, Mitochondrial

complex II: at the crossroads, Trends Biochem. Sci. 42 (2017) 312–325.
[23] M. Davoudi, H. Kotarsky, E. Hansson, V. Fellman, Complex I function and supercomplex formation are preserved in liver mitochondria despite progressive complex III deficiency, PLoS One 9 (2014) e86767.
[24] M. Tonkonogi, K. Sahlin, Rate of oxidative phosphorylation in isolated mitochondria from human skeletal muscle: effect of training status, Acta Physiol. Scand. 161 (1997) 345–353.
[25] M. Hey-Mogensen, M. Gram, M.B. Jensen, M.T. Lund, C.N. Hansen, M. Scheibye-Knudsen, V.A. Bohr, F. Dela, A novel method for determining human ex vivo submaximal skeletal muscle mitochondrial function, J. Physiol. 593 (2015) 3991–4010.
[26] S. Maekawa, D. Mori, T. Nishiya, O. Takikawa, T. Horinouchi, A. Nishimoto, E. Kajita, S. Miwa, OCTN2VT, a splice variant of OCTN2, does not transport carnitine because of the retention in the endoplasmic reticulum caused by insertion of 24 amino acids in the first extracellular loop of OCTN2, Biochim. Biophys. Acta 1773 (2007) 1000–1006.
[27] L.B. Christiansen, F. Dela, J. Koch, C.N. Hansen, P.S. Leifsson, T. Yokota, Impaired cardiac mitochondrial oxidative phosphorylation and enhanced mitochondrial oxidative stress in feline hypertrophic cardiomyopathy, Am. J. Physiol. Heart Circ. Physiol. 308 (2015) H1237–H1247.
[28] W. Mizushima, H. Takahashi, M. Watanabe, S. Kinugawa, S. Matsushima, S. Takada, T. Yokota, T. Furihata, J. Matsumoto, M. Tsuda, I. Chiba, S. Nagashima, S. Yanagi, M. Matsumoto, K.I. Nakayama, H. Tsutsui, S. Hatakeyama, The novel heart-specific RING finger protein 207 is involved in energy metabolism in cardiomyocytes, J. Mol. Cell. Cardiol. 100 (2016) 43–53.
[29] S. Maekawa, S. Takada, H. Nambu, T. Furihata, N. Kakutani, D. Setoyama, Y. Ueyanagi, D. Kang, H. Sabe, S. Kinugawa, Linoleic acid improves assembly of the CII subunit and CIII2/CIV complex of the mitochondrial oxidative phosphorylation system in heart failure, Cell Commun. Signal. 17 (2019) 128.
[30] H. Nambu, S. Takada, A. Fukushima, J. Matsumoto, N. Kakutani, S. Maekawa, R. Shirakawa, I. Nakano, T. Furihata, T. Katayama, K. Yamanashi, Y. Obata, A. Saito, T. Yokota, S. Kinugawa, Empagliflozin restores lowered exercise endurance capacity via the activation of skeletal muscle fatty acid oxidation in a murine model of heart failure, Eur. J. Pharmacol. (2019) 172810.
[31] D.S. Lark, M.J. Torres, C.T. Lin, T.E. Ryan, E.J. Anderson, P.D. Neufer, Direct real-time quantification of mitochondrial oxidative phosphorylation efficiency in permeabilized skeletal muscle myofibers, Am. J. Physiol. Cell Physiol. 311 (2016) C239–C245.
[32] C.M. Julienne, J.F. Dumas, C. Goupille, M. Pinault, C. Berri, A. Collin, S. Tesseraud, C. Couet, S. Servais, Cancer cachexia is associated with a decrease in skeletal muscle mitochondrial oxidative capacities without alteration of ATP production efficiency, J. Cachexia Sarcopenia Muscle 3 (2012) 265–275.
[33] G. Quarato, C. Piccoli, R. Scrima, N. Capitanio, Variation of flux control coefficient of cytochrome c oxidase and of the other respiratory chain complexes at different values of protonmotive force occurs by a threshold mechanism, Biochim. Biophys. Acta 1807 (2011) 1114–1124.
[34] S. Smith, I.R. Cottingham, C.I. Ragan, Immunological assays of the NADH dehydrogenase content of bovine heart mitochondria and submitochondrial particles, FEBS Lett. 110 (1980) 279–282.
[35] Y. Hatefi, The mitochondrial electron transport and oxidative phosphorylation system, Annu. Rev. Biochem. 54 (1985) 1015–1069.
[36] R.A. Capaldi, D.G. Halphen, Y.Z. Zhang, W. Yanamura, Complexity and tissue specificity of the mitochondrial respiratory chain, J. Bioenerg. Biomembr. 20 (1988) 291–311.
[37] H. Schagger, K. Pfeiffer, The ratio of oxidative phosphorylation complexes I-V in bovine heart mitochondria and the composition of respiratory chain supercomplexes, J. Biol. Chem. 276 (2001) 37861–37867.
[38] A.S. Hoekstra, J.P. Bayley, The role of complex II in disease, Biochim. Biophys. Acta 1827 (2013) 543–551.